Delocalization, thermal ionization, and energy transfer in singly doped and codoped CaAl₄O₇ and Y₂O₃

Dongdong Jia,[1] Xiao-jun Wang,[2,3,*] and W. M. Yen[4]

[1]*Department of Physics, University of Puerto Rico, Mayaguez, Puerto Rico 00681, USA*

[2]*Key Laboratory of Excited State Processes, Changchun Institute of Optics, Fine Mechanics, and Physics, Chinese Academy of Sciences, Changchun 130033, People's Republic of China*

[3]*Department of Physics, Georgia Southern University, Statesboro, Georgia 30460, USA*

[4]*Department of Physics & Astronomy, University of Georgia, Athens, Georgia 30602, USA*

Ce^{3+} and Tb^{3+} singly doped and codoped CaAl₄O₇ and Y₂O₃ single crystal fibers were grown using the laser heated pedestal growth method. Energy transfer from Ce^{3+} to Tb^{3+} was studied in these samples. No energy transfer between Ce^{3+} and Tb^{3+} was observed in codoped Y₂O₃. This is because electrons excited into the Ce^{3+} $5d$ states delocalize into the conduction band at a rate that is faster than the interionic energy transfer rate, whereas the converse is the case for CaAl₄O₇ doped with Ce^{3+} (1 at %) and Tb^{3+} (1 at %). The energy transfer rate was determined to be on the order of 10^9 s^{-1}. The transfer occurs before the excited electrons can be thermally promoted into the conduction band. From these results, it can be inferred that the thermal ionization rate (W_{Th}) from the lowest $5d$ excited Ce^{3+} state at 355 nm is less than 10^9 s^{-1} at room temperature, whereas the delocalization rate (W_D) into the conduction band is faster than this rate. The location of the Tb^{3+} and Ce^{3+} states relative to the valence and conduction band of these two materials has been determined through photoconductivity measurements.

I. INTRODUCTION

In practical applications, such as phosphors and solid-state lasers, rare earth ions are frequently used as doped activators.[1–3] The behavior of the active electrons of these ions in their excited state is important in determining the properties of the materials.

The spectra of the rare earth ions are dominated by intrastate, $4f$ to $4f$, transitions which generally consist of sharp line spectra largely insensitive to the crystalline hosts. These properties are inherent to the nature of the $4f$ states which are well shielded from external perturbations. Electrons in $4f$ states are localized and can be designated to specific impurity ions.

The first set of interconfigurationally allowed states are the $5d$ states, which are more extensive physically and hence interact more strongly with the surrounding ligands when in a solid. As a consequence, the $4f$ to $5d$ transitions are broad and can vary in energy considerably. The position of the $5d$ states of rare earth ions has been extensively studied specially for Ce^{3+}.[4] Because of their extent, $5d$ states are sensitive to crystalline field changes, and $5d$ field components can be energy resonant with the conduction band of the host. Electrons promoted to $5d$ states can become conduction electrons under the proper circumstances, resulting in the loss or delocalization of the electrons from the impurity ion. In other words, the impurity ion can be photoionized through $5d$ excitation. Photoionization can be also thermally induced if optically excited states are below the conduction band but sufficiently close to it. If the state in question is emissive, thermal photoionization competes with the radiative process and affects the overall luminescence quantum efficiency of the state.[5]

Because of the simple energy level structure the $(4f)^1$ configuration, the spectroscopic properties of Ce^{3+} in various hosts have been studied extensively.[6] Special emphasis has been placed on the nature of the $5d$ states which are affected by the symmetry and strength of the crystalline field of the host matrix.[7] For cubic symmetry, the $5d^1$ state will split into E and T states. For both Y₂O₃ and CaAl₄O₇ systems, the symmetries of Y^{3+} and Ca^{2+} sites are lower (the two Y^{3+} sites of symmetry C_2 and C_{3i} and one Ca^{2+} site of symmetry C_2),[8,9] causing further splitting of the E and T states. For Y₂O₃, the $5d$ components fall within the conduction band, while in the case of CaAl₄O₇ the lowest $5d$ multiplet lies below the conduction band. The position of the lowest component of the $5d$ states determines the radiative behavior of Ce^{3+} in a given material. For example, no $5d$-$4f$ luminescence is observed in Y₂O₃, while strong broadband transitions are observed in the Ca compound.[10–12] This is a consequence of the delocalization of the electron while in the conduction band.

Ce^{3+} has been established as a luminescence sensitizer for the Tb^{3+} ion. The energy transfer process leading to the enhancement of the Tb^{3+} $4f$-$4f$ transition originates from the metastable lowest $5d$ state of the Ce^{3+} ion, and under the proper conditions, the energy transfer rate can be high enough to change the emission dynamics of the donor state. In the doubly doped system, interionic energy transfer provides an additional competing mechanism for the de-excitation of the Ce^{3+} state. The various mechanisms involved are schematically depicted in Fig. 1, including direct radiative decay back to the ground state, direct and thermally induced photoionization (delocalization), and the process of sensitization (energy transfer). Typically for rare earth systems, the radiative decay rate for a $5d$ to $4f$ transition (W_d) is
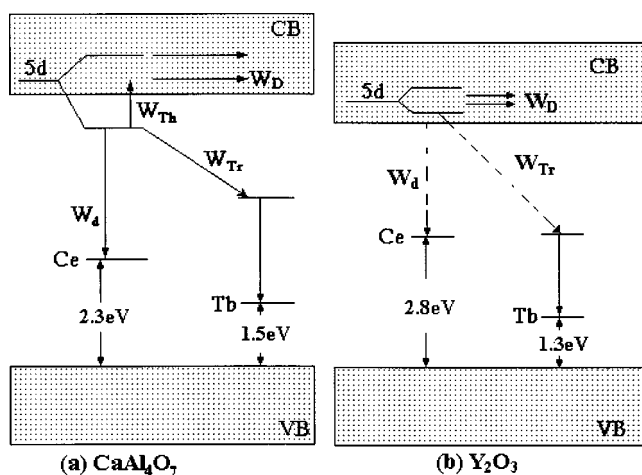
FIG. 1. Energy diagram of (a) $CaAl_4O_7:Tb^{3+},Ce^{3+}$ and (b) $Y_2O_3:Tb^{3+},Ce^{3+}$. W_d is the decay rate of 355 nm $5d$ level of Ce^{3+}, W_{Tr} the energy transfer rate from Ce^{3+} to Tb^{3+}, W_{Th} the thermal ionization rate, and W_D the delocalization rate (solid lines: occurred; dashed lines: did not occur).
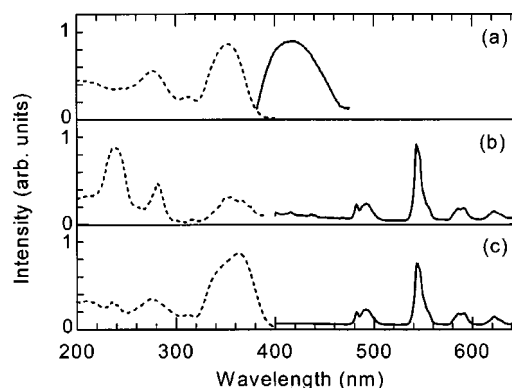

FIG. 2. Emission (solid lines) and excitation (dashed lines) spectra of the samples. All emissions are recorded upon excitation at 355 nm. The excitation spectra are monitored at 420, 542.9, and 542.9 nm for (a) $CaAl_4O_7:Ce^{3+}$, (b) $CaAl_4O_7:Tb^{3+}$, and (c) $CaAl_4O_7:Tb^{3+},Ce^{3+}$, respectively.

of the order of 10^7 s^{-1}; the energy transfer rate can be controlled by adjusting the concentrations of donor and acceptor, i.e., distance between the donors and acceptors.

In this work, by comparing the dynamic behavior of the Ce^{3+} excitation in the doubly doped systems and contrasting the competing de-excitations mechanisms for the $5d$ state, we find that we can make estimates for the thermal ionization rate (W_{Th}) and the delocalization rate (W_D) for rare earth electrons occupying the Ce^{3+} states. The thermal ionization rate (W_{Th}) is analogous to the spin-lattice relaxation rate and is a measure of the strength of the electron-phonon interaction of the excited $5d$ states of rare earth ions with the host.

II. EXPERIMENT

The $Y_2O_3:Ce^{3+}$, $Y_2O_3:Tb^{3+}$, $Y_2O_3:Tb^{3+},Ce^{3+}$, and $CaAl_4O_7:Ce^{3+}$, $CaAl_4O_7:Tb^{3+}$, $CaAl_4O_7:Tb^{3+},Ce^{3+}$, single crystal fibers were prepared by the laser heated pedestal growth (LHPG) method.[13] Pellets of the starting mixture were made with the proper mole ratio. The doping concentration is 1 at % for all dopants. The pellets were sintered at 1200 °C in air in a Linderburg blue tube furnace for 2 h and were cut and milled into 1-mm square rods with (without) a sharp tip to serve as the seed (feed). The samples were reduced at 1350 °C in a 5° H_2+N_2 gas flow. This is necessary because both Ce^{4+} and Tb^{4+} are also stable valence states. The fiber samples were polished into thin slabs (200–300 -μm thickness) along their fiber axis with two parallel end surfaces.

Photoconductivity spectra of the samples were measured at room temperature (290 K) and at 140 K. Ni meshes served as the electrodes. The light source was an Oriel 200 W Xenon lamp filtered through an ISA Jobin Yvon Spex monochromator. The samples were mounted in an electrically and thermally shielded vacuum cryostat. The applied voltage was about 10 000 V/cm. A Keithley 6517A elec-

trometer was used both as the high voltage supply and as the current detector.

The fluorescence lifetimes were recorded using a Tektronix 460A digital oscilloscope and a SPEX M500 spectrometer upon excitation with a frequency tripled Nd:YAG laser (pulse width ~7.0 ns). The other optical measurements such as emission and excitation spectra were taken with a SPEX FluoroMax spectrofluorimeter. The band gaps of Y_2O_3 and $CaAl_4O_7$ are determined from the optical absorption to be 5.6 and 6.2 eV, respectively, using undoped samples.

III. RESULTS AND DISCUSSION

A. Energy transfer and thermal ionization in $CaAl_4O_7$ samples

Figure 2 shows the emission (solid) and excitation (dashed) spectra of the $CaAl_4O_7$ samples doped with Ce^{3+} and Tb^{3+} individually [Figs. 2(a) and 2(b)] and jointly [Fig. 2(c)]. The doping concentration of the samples was nominally 1 at % for both dopant ions. The excitation spectra were obtained by monitoring emissions peaks for Ce^{3+} [420 nm, Fig. 2(a)] and Tb^{3+} [542.9 nm, Figs. 2(b) and 2(c)], respectively. The emission spectra were measured upon excitation at 355 nm corresponding to peak of the Ce^{3+} absorption.

For the singly Ce^{3+} doped samples, the excitation spectra consist of multiplets of the $5d$ state. The lowest $5d$ state peaking at 355 nm lies below the conduction band of $CaAl_4O_7$. The excitation spectra of Tb^{3+} consist of high lying $4f$ states as well as components of its $5d$ states.

The emission of Ce^{3+} in the codoped sample disappeared upon excitation at 355 nm, and the features of Ce^{3+} excitation appear in the excitation spectrum of Tb^{3+} when monitored at Tb^{3+} 542.9-nm emission. These facts indicate that energy transfer from Ce^{3+} to Tb^{3+} in the codoped sample takes place. The lifetime of the Ce^{3+} emission in the singly doped sample is measured to be 35 ns. In the codoped sample, it is greatly shortened and is not detectable by using an excitation pulse of 7 ns pulse width; this implies that the
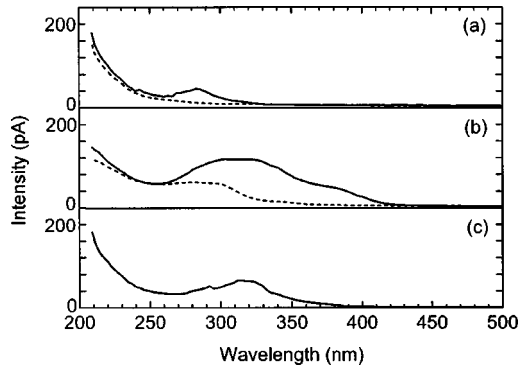
FIG. 3. Photoconductivity spectra of the CaAl$_4$O$_7$ samples: (a) CaAl$_4$O$_7$:Tb^{3+}; (b) CaAl$_4$O$_7$:Ce^{3+}; (c) CaAl$_4$O$_7$:Tb^{3+},Ce^{3+} (solid lines: 290 K; dashed lines: 140 K).

energy transfer rate, W_{Tr}, is $\sim 10^9$ s^{-1} at 1 at % concentration and that is much faster than the Ce^{3+} emission rate, W_d, which is of the order of 10^7 s^{-1}. The energy transfer occurs from the lowest 5d band of Ce^{3+} (at 355 nm). It depletes the population of lowest Ce^{3+} state rapidly and reduces the probability of thermal promotion to the conduction band. Details will be discussed in the section below.

Photoionization depends largely on the relative position of the impurity energy levels to the host band gap. Photoconductivity measurements are helpful in determining the impurity band positions relative to the host band gap, and in studying the thermal ionization of the excited state electrons. A photocurrent is observed as the electrons from impurities reach the conduction band. The photocurrent spectra are correlated to the excitation spectra of the electrons in the conduction band. If the excited states lie below the conduction band, then the photocurrent spectra will depend on the thermal ionization rate W_{Th} that is given in form of

$$W_{Th} = s e^{-\Delta E/kT}, \tag{1}$$

where ΔE is the energy deference between conduction band and the excited states below and s is a frequency factor, similar to that defined for thermal quenching.[14]

If thermal ionization is involved, the excitation spectra, and the photocurrent spectra will have some differences. The photocurrent of the excited states below the conduction band will be weaker than the excitation spectra, because fewer electrons are being promoted to the conduction band. THC thermal dependence of the ionization process is such that at lower temperatures the onset of the photocurrent signal shifts to higher energies, and hence the energy splitting can be determined by using the two onset energies at two temperatures.

The photoconductivity spectra of the Ce^{3+} and Tb^{3+} singly- and codoped CaAl$_4$O$_7$ samples are shown in Fig. 3. Tb^{3+} ions generate very weak photocurrent in the sample, as shown in Fig. 3(a). A photocurrent peak of Tb^{3+} is found at 283 nm and is assigned to the lowest 5d states of Tb^{3+}. From the onsets at two temperatures (140 and 290 K) in Fig. 3 and assuming the photocurrent proportional to thermal ionization rate and emission intensity at the same wavelength, the energy difference between the conduction band and 5d band at

283 nm for Tb^{3+} is estimated to be 0.33 eV. Taking the measured band gap value of CaAl$_4$O$_7$ as 6.2 eV, the ground state of Tb^{3+} then can be placed 1.5 eV above the valence band, as shown in Fig. 1. No photocurrent signals were observed in the Tb^{3+} 4f-4f transition region.

The Ce^{3+} photocurrent spectra are shown in Fig. 3(b). At room temperature, the Ce^{3+} photocurrent spectrum agrees with the Ce^{3+} excitation spectrum. An interesting observation is that the photocurrent intensity is found to be weak while the excitation intensity is strong at 355 nm. A possible explanation is that thermal ionization occurs at the 355 nm (5d band), which means that the 5d band of Ce^{3+} is below the host conduction band. In addition, the onset of the photocurrent spectrum shifts to higher energy at low temperature (140 K), also indicating that thermal ionization is occurring. The 5d band at 355 nm is estimated to be ~ 0.3 eV below the host conduction band calculated from the two onset energies at two temperatures. Hence, the Ce^{3+} ground state is about 2.3 eV above the host valence band (see Fig. 1). The positions of the other energy levels of the Tb^{3+} and Ce^{3+} relative to the host band gap can then be determined by these optical transition energies as determined by spectroscopy.

The photocurrent of the codoped sample is similar to the Ce^{3+} singly doped samples. The Tb^{3+} photocurrent is too weak to be detected in these samples. The photocurrent behavior at lower energies of the Ce^{3+} 5d level is very interesting; it is clearly much weaker than that of the singly doped sample. This indicates that energy transfer from Ce^{3+} to Tb^{3+} is occurring and that the electron population at the 5d state is being reduced quickly. Because of this, fewer electrons are available to be promoted to the conduction band through ionization. The thermal ionization rate W_{Th} of the electrons in the Ce^{3+} 5d band is slower than the energy transfer rate $W_{Tr}(\sim 10^9$ s$^{-1})$.

Based on the discussion above, W_{Th} can be estimated in between W_d (10^7 s^{-1} or greater for singly doped Ce^{3+}) and W_{Tr}. The frequency factor s can then be estimated to be of the order of 10^{12} s^{-1}, while the frequency factor of thermal detrapping process s_d in a similar host CaAl$_2$O$_4$ has been found to be 10^{8-9} s^{-1},[15,16] which is very different from the s value in CaAl$_4$O$_7$.

B. Energy transfer and delocalization in Y$_2$O$_3$

There is no Ce^{3+} emission is observed in Y$_2$O$_3$.[10] The Tb^{3+} excitation and emission spectra are shown in Fig. 4(a). The strong 4f-5d transition of Tb^{3+} is found at 310 nm, while f-f transitions are observed at 492, 542.9, 590, and 630 nm, respectively. Ce^{3+} and Tb^{3+} were also codoped in Y$_2$O$_3$, and their emission and excitation spectra are shown in Fig. 4(b). The emission and excitation spectra of the Tb^{3+} singly doped and codoped with Ce^{3+} samples are identical and imply that there is no energy transfer from Ce^{3+} to Tb^{3+} in this host. There is no absorption observed around 390 nm [that appears in the photocurrent spectrum in Fig. 5(c)] in the excitation spectrum when monitoring Tb^{3+} emission.

Photocurrent spectra of all three samples are shown in Fig. 5. The photocurrent of Tb^{3+} 5d states at 310 nm is quenched at low temperature because this state is below the
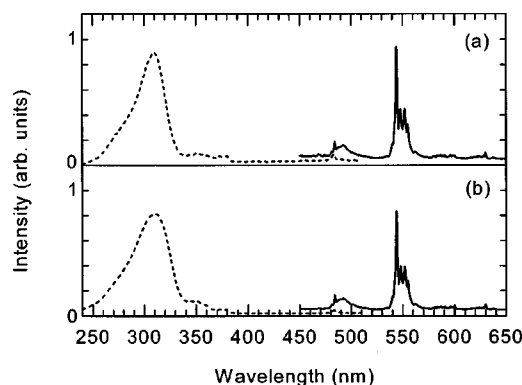
FIG. 4. Emission (solid lines) and excitation (dashed lines) spectra of the samples. Both emissions are recorded upon excitation at 310 nm and both excitation spectra are monitored at 542.9 nm. (a) Y_2O_3:Tb^{3+} and (b) Y_2O_3:Tb^{3+},Ce^3.

conduction band. The onsets of photocurrent signals of Tb^{3+} are found at 324 nm (290 K) and 306 nm (140 K) as shown in Figs. 5(a) and 5(b). It follows that the $5d$ band of Tb^{3+} at 310 nm is estimated 0.25 eV below the Y_2O_3 conduction band. Using the measured band gap value of Y_2O_3 as 5.6 eV, the ground state of Tb^{3+} can be placed at 1.3 eV above the Y_2O_3 valence band. In the codoped sample, photocurrent peaks from both Tb^{3+} and Ce^{3+} are observed in Fig. 5(c) at room temperature. The Ce^{3+} photocurrent peak is found at 390 nm. The Ce^{3+} $5d$ bands are all in the conduction band, and its ground state is hence about 2.8 eV above the Y_2O_3 valence band (see Fig. 1).

The Ce^{3+} emission is quenched by electron delocalization in Y_2O_3 because all the $5d$ bands are above the host conduction band. These delocalized electrons relax to the bottom of the conduction band. The Ce^{3+} emission rate W_d is normally 10^7 s^{-1}, so that the delocalization rate W_D in Y_2O_3 must be faster than 10^7 s^{-1} in order to quench the Ce^{3+} emission.

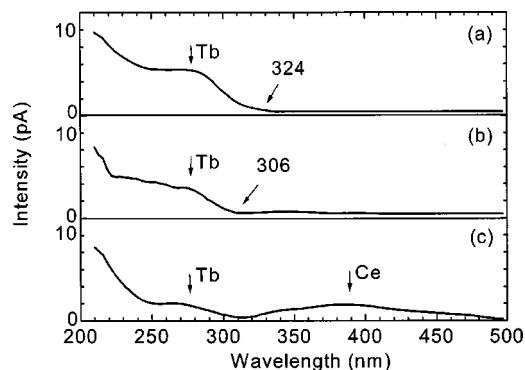FIG. 5. Photoconductivity spectra: (a) Y_2O_3:Tb^{3+} at 290 K; (b) Y_2O_3:Tb^{3+} at 140 K; and (c) Y_2O_3:Tb^{3+},Ce^3 at 290 K.

In general, the energy transfer rate from Ce^{3+} to Tb^{3+} is of the order of 10^8–10^9 s^{-1}. The Ce^{3+} to Tb^{3+} energy transfer is mostly due to a dipole-dipole interaction which depends on the donor-acceptor distance $R(\propto 1/R^6)$. Under the same doping concentration, the distance R between Ce^{3+} and Tb^{3+} is smaller in Y_2O_3 than that in $CaAl_4O_7$, so that the energy transfer rate between Ce^{3+} and Tb^{3+} should be greater in Y_2O_3 than in $CaAl_4O_7$; the latter rate was estimated of the order of 10^9 s^{-1} at 1 at % doping concentration (it is far less than the quenching concentration).[17] The reason for the absence of energy transfer in Y_2O_3 is that all the $5d$ components are in the conduction band and the delocalization rate is much faster than the energy transfer rate, i.e., $W_D \gg W_{Tr}(\sim 10^9$ s$^{-1})$. Once the electrons are excited to the $5d$ states from the ground state, they delocalize to generate photocurrent, instead of engaging in the transfer of energy to Tb^{3+} to yield emission.

IV. CONCLUSION

We have studied two sets of samples, $CaAl_4O_7$:Tb^{3+}/Ce^{3+}/Tb^{3+},Ce^{3+} and Y_2O_3:Tb^{3+}/Ce^{3+}/Tb^{3+},Ce^{3+}. The energy transfer rate, W_{Tr}, from Ce^{3+} to Tb^{3+} is of the order of 10^9 s^{-1} in both $CaAl_4O_7$ and Y_2O_3 systems. The Tb^{3+} and Ce^{3+} ground-state positions relative to hosts' band gap were determined by photoconductivity measurement. The Tb^{3+} ground state is 1.5 and 1.3 eV above the $CaAl_4O_7$ and Y_2O_3 valence band, respectively. The Ce^{3+} ground state is 2.3 and 2.8 eV above the $CaAl_4O_7$ and Y_2O_3 valence band, respectively.

The thermal ionization process of the Ce^{3+} ion is observed in $CaAl_4O_7$. A competition between thermal ionization and energy transfer is observed and allows us to estimate various rates. Thermal ionization of the $5d$ electrons of Ce^{3+} at 355 nm is dominated by the energy transfer process from Ce^{3+} to Tb^{3+} in $CaAl_4O_7$. The thermal ionization rate (W_{Th}) at 355-nm $5d$ level at 290 K in $CaAl_4O^7$ is estimated in the range of $W_{Tr}(\sim 10^9$ s$^{-1}) > W_{Th} \sim W_d(\sim 10^7$ s$^{-1})$.

Delocalization of the $5d$ electrons of Ce^{3+} ions in Y_2O_3 is a dominant process in the de-excitation. The energy transfer from Ce^{3+} to Tb^{3+} is quenched by the delocalization of the $5d$ electrons of Ce^{3+} in Y_2O_3. The delocalization, energy transfer, and radiation rates are found to have the following relationship: $W_D > W_{Tr}(\sim 10^9$ s$^{-1}) > W_d(\sim 10^7$ s$^{-1})$.

*Electronic address: xwang@georgiasouthern.edu

[1] S. Tanimizu, in *Phosphor Handbook*, edited by S. Shionoya and W. M. Yen (CRC Press, Boca Raton, 1999), p. 153.

[2] T. Schweizer, T. Jensen, E. Heumann, and G. Huber, Opt. Commun. **118**, 557 (1995).

[3] D. S. Hamilton, S. K. Gayen, G. J. Pogatshnik, R. D. Ghen, and W. J. Miniscalco, Phys. Rev. B **39**, 8807 (1989).

[4] D. Jia, R. S. Meltzer, and W. M. Yen, J. Lumin. **99**, 1 (2002).

[5] W. M. Yen, J. Lumin. **83-84**, 399 (1999).

[6] P. Dorenbos, J. Lumin. **91**, 155 (2000); **91**, 91 (2000).

[7] P. Dorenbos, J. Phys.: Condens. Matter **15**, 6249 (2003).

[8] R. M. Ranson, E. Evangelou, and C. B. Thomas, Appl. Phys. Lett. **72**, 2663 (1998).

[9] H. Yuan, W. M. Dennis, L. Lu, W. Jia, H. Liu, and W. M. Yen, in *Proceedings of the Sixth International Conference on Luminescent Materials*, Paris, 1997, edited by R. Ronda and T. Welker, Electrochem. Soc. Proc., Vol. 97-29 (The Electrochemical Society, Inc., Pennington, NJ, 1998), p. 206.

[10] M. Raukas, "Luminescence efficiency and electronic properties of cerium doped insulating oxides," thesis (The University of Georgia, 1997).

[11] D. Jia, W. Jia, R. S. Meltzer, W. M. Yen, and X. J. Wang, Appl. Phys. Lett. **80**, 1535 (2002).

[12] M. V. Hoffman, J. Electrochem. Soc. **118**, 1508 (1971).

[13] B. M. Tissue, L. Lu, W. Jia, and W. M. Yen, J. Cryst. Growth **109**, 323 (1991).

[14] H. Yamamoto, in *Phosphor Handbook*, edited by S. Shionoya and W. M. Yen (CRC Press, Boca Raton, 1999), p. 38.

[15] S. W. S. McKeever, *Thermoluminescence in Solid* (Cambridge University Press, Cambridge, 1985), p. 5.

[16] D. Jia and W. M. Yen, J. Electrochem. Soc. **150**, H61 (2003).

[17] W. M. Li and M. Leskela, Mater. Lett. **28**, 491 (1996).